SUPPLEMENTARY MATERIALS
to the article by N.S. Dyrkheeva, I.A. Chernyshova, A.F. Arutyunyan, A.L. Zakharenko, M.M. Kutuzov, K.N. Naumenko, A.S. Venzel, V.A. Ivanisenko, S.M. Deyev, A.L. Zhuze, O.I. Lavrik
"The effect of dimeric bisbenzimidazoles on the activity of DNA repair enzymes TDP1, TDP2, PARP1 and PARP2"

Table S1. RMSD table for dimeric inhibitors $DB_2Py(n)$ and $DB_2P(n)$ in complex with TDP1 relative to the optimal conformation of the base fragment

Inhibitor name	Monomeric unit name	Number of poses obtained	Best GridScore, kcal/mol	RMSD range, Å	Selected pose number	RMSD of selected pose, Å
$DB_2Py(1)$	$MB_2Py(Ac)$	5	–109.49	10.6–23.2	2	10.6
$DB_2Py(3)$		10	–113.92	5.7–23.2	1	11.5
$DB_2Py(4)$		8	–111.54	8.2–26.8	2	8.2
$DB_2Py(5)$		4	–116.65	11.7–24.1	1	11.7
$DB_2Py(7)$		6	–124.69	11.6–25.8	5	11.6
$DB_2Py(9)$		5	–131.12	8.5–27.1	1	8.5
$DB_2Py(11)$		3	–126.10	8.5–26.9	1	8.5
$DB_2P(1)$	$MB_2(Ac)$	6	–104.47	9.9–20.6	3	9.9
$DB_2P(2)$		4	–105.51	12.6–17.1	1	12.6
$DB_2P(3)$		2	–112.57	11.8–14.1	1	11.8
$DB_2P(4)$		6	–112.11	11.3–19.2	5	11.3

RMSD values were calculated between the base compound and the nearest monomeric fragment of the dimeric compound, accounting for fragment orientation without changing molecular coordinates. Calculations were performed using the RDKit package.

Table S2. Binding scores for dimeric inhibitors $DB_2Py(n)$ and $DB_2P(n)$ with TDP1

Inhibitor name	DOCK ContinuousScore, kcal/mol	X-Score, pKd	Vinardo, kcal/mol	Ref2015, REU
$DB_2Py(1)$	–78.0	7.55	–9.05	–14.77
$DB_2Py(3)$	–88.2	7.91	–11.21	–16.28
$DB_2Py(4)$	–82.2	8.06	–10.04	–18.04
$DB_2Py(5)$	–92.7	8.07	–11.61	–16.94
$DB_2Py(7)$	–93.5	8.18	–11.40	–18.52
$DB_2Py(9)$	–101.2	8.40	–12.38	–21.24
$DB_2Py(11)$	–101.1	8.04	–11.10	–20.93
$DB_2P(1)$	–82.6	7.08	–8.94	–18.62
$DB_2P(2)$	–82.2	7.03	–9.05	–18.22
$DB_2P(3)$	–86.3	7.49	–10.97	–18.12
$DB_2P(4)$	–86.1	7.01	–9.92	–16.37

DOCK ContinuousScore – energy scoring of the complex in UCSF DOCK 6.11 without grid construction, including van der Waals and Coulombic interactions after ligand minimization in the binding site. Vinardo Score – an empirical function accounting for hydrogen bonds, hydrophobic and van der Waals interactions with calibration against experimental data. X-Score – average value across three components for assessing hydrophobic, polar, and electrostatic contacts. The all-atom energy scoring function Ref2015 (PyRosetta) combines van der Waals, electrostatic, hydrogen bonding, and solvation interactions for high-precision complex evaluation. In assessing ligand binding affinity to TDP1, more negative values for Vinardo, Ref2015, and DOCK ContinuousScore indicate higher interaction affinity. Conversely, for X-Score, higher values reflect greater binding strength, as this function uses a scale where positive scores correlate with better affinity.

Molecular Dynamics Protocol

Investigation of the dynamics of the TDP1 protein-ligand complex with $DB_2Py(1)$ was performed using molecular dynamics with the OpenMM 8 software package.

The AMBER ff14SB force field was applied for protein parameterization, and the GAFF-2.11 force field was used for the ligand using the OpenFF Toolkit. During simulation, the complex was placed in a cubic box with TIP3P water molecules, with a minimum distance of 10 Å from complex atoms to box boundaries. The boundaries were periodic. The system charge was neutralized by adding Na^+ and Cl^- ions to achieve physiological ionic strength.

Hydrogen mass repartitioning (4 a.m.u.) was applied to increase the integration timestep to 2 fs. After energy minimization, system equilibration was conducted for 0.1 ns at 300 K. The simulation duration was 10 ns.

Temperature was maintained at 300 K using a Langevin thermostat (friction coefficient 1.0 ps^{-1}), and pressure at 1 atm using a Monte Carlo barostat with volume adjustment every 25 steps. Bonds involving hydrogen atoms were constrained using the SHAKE algorithm. System coordinates were saved every 10 ps.

Trajectory analysis was performed using the MDTraj package.

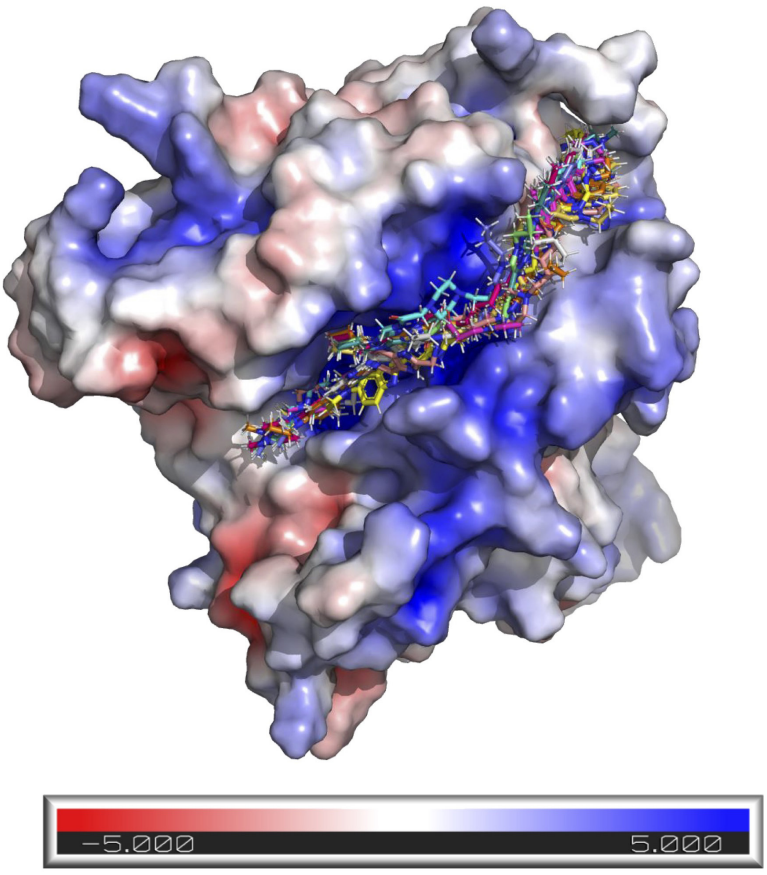

Fig. S1. Predicted conformations of inhibitors $DB_2Py(n)$ and $DB_2P(n)$ on the TDP1 surface (PDB ID: 8V0B).

The protein surface is colored according to the electrostatic potential distribution calculated using APBS (Jurrus et al., 2018). Color scale: red – negative potential (–5 kT/e), white – neutral (0 kT/e), blue – positive potential (+5 kT/e).

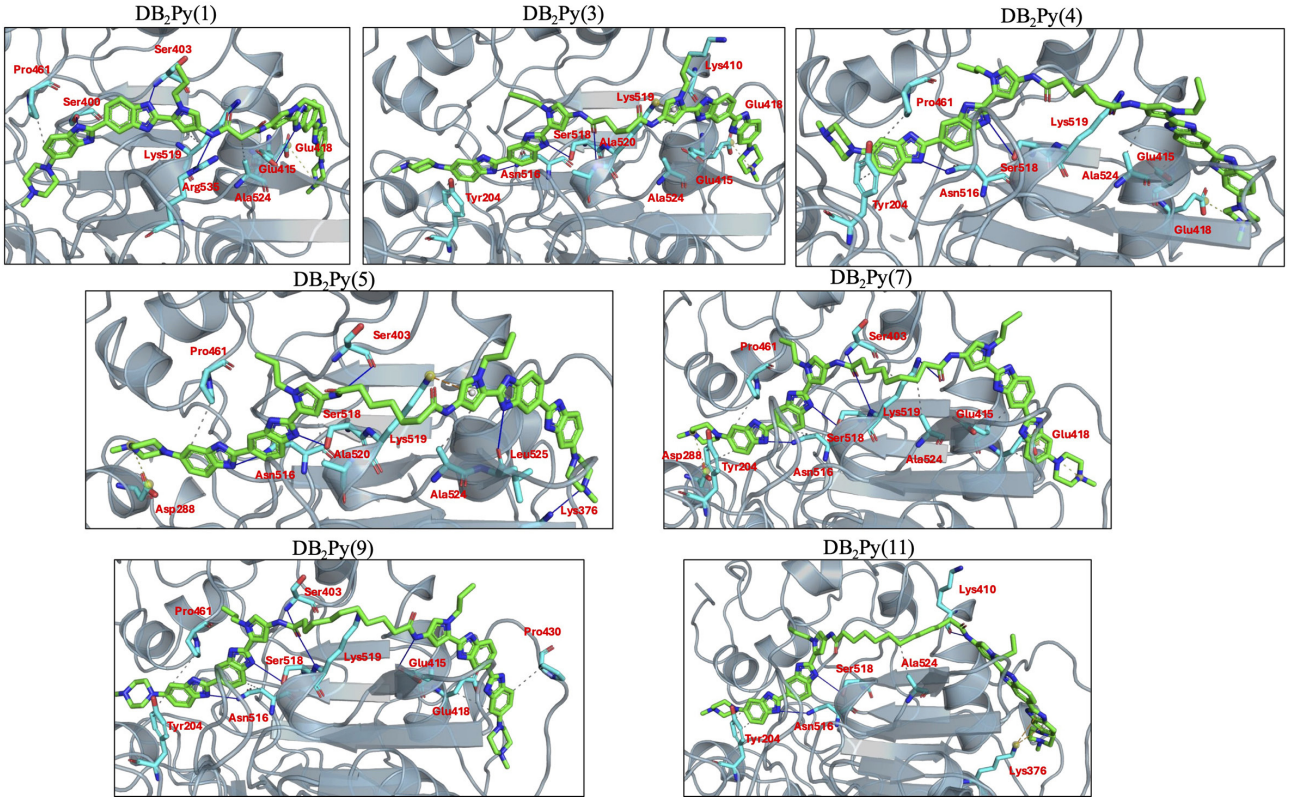

Fig. S2. Predicted conformations of $DB_2Py(n)$ family inhibitors in complex with TDP1 with interacting residues.

Solid blue lines – hydrogen bonds, gray dashed lines – hydrophobic interactions, orange dashed lines – pi-cation interactions, yellow dashed lines – salt bridges.

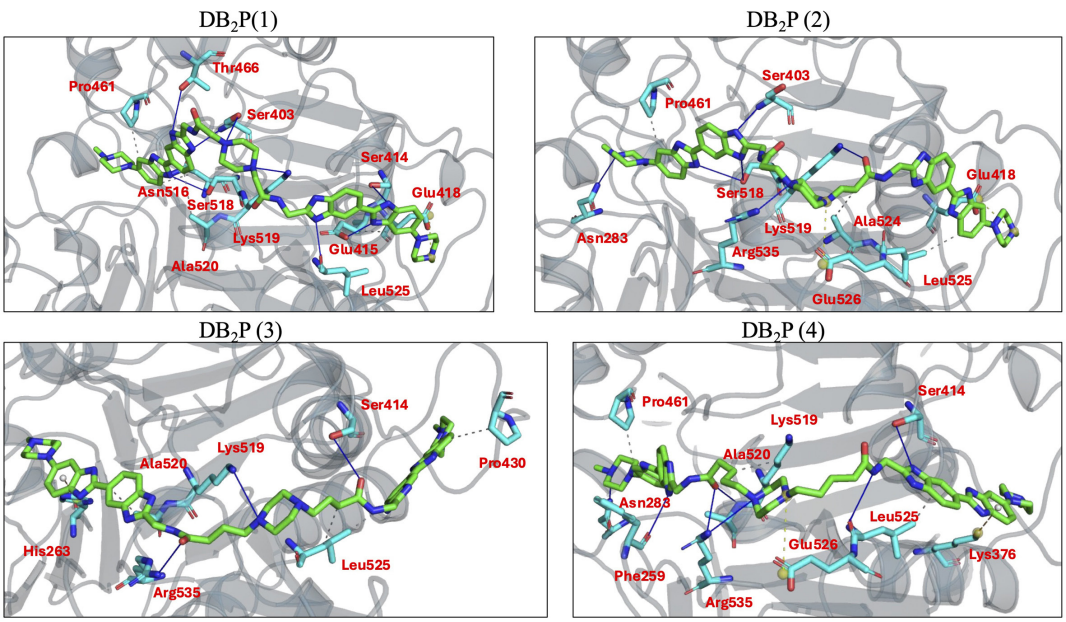

Fig. S3. Predicted conformations of $DB_2P(n)$ family inhibitors in complex with TDP1 with interacting residues.

Solid blue lines – hydrogen bonds, gray dashed lines – hydrophobic interactions, orange dashed lines – pi-cation interactions, yellow dashed lines – salt bridges.

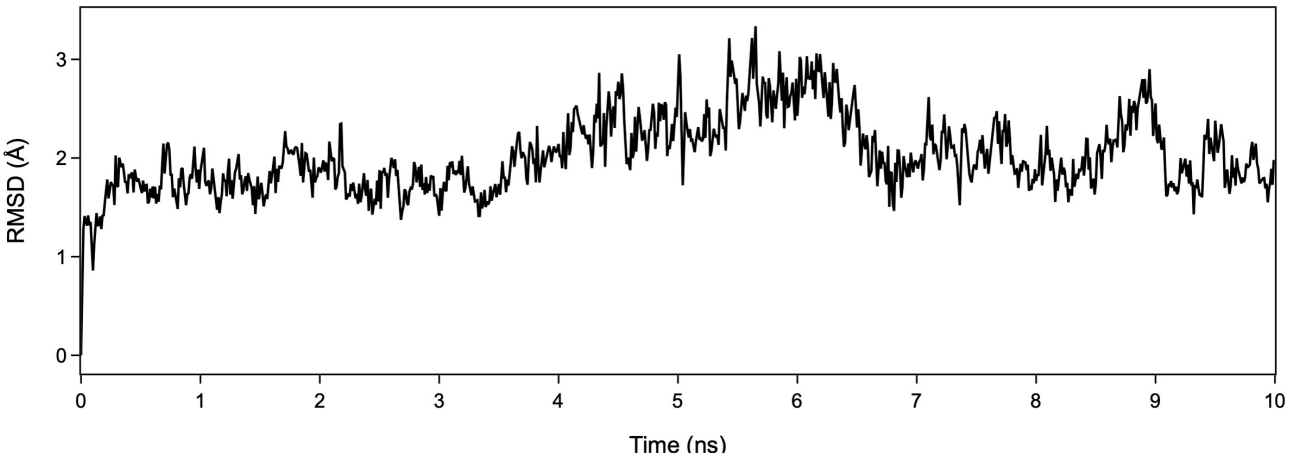

Fig. S4. Root mean square deviation (RMSD) analysis of $DB_2Py(1)$ position in the protein active site during 10-ns molecular dynamics simulation.

The graph demonstrates the temporal evolution of ligand RMSD relative to its initial conformation after protein structure superposition. RMSD values fluctuate in the range of 1.5–3.0 Å, indicating stable ligand binding to the protein throughout the entire simulation trajectory. After the initial equilibration period (0–200 ps), relatively stable system behavior is observed with an average RMSD value of approximately 2.0–2.5 Å. Periodic RMSD fluctuations indicate conformational mobility of the ligand within the active site while maintaining key interactions with the protein. The absence of sharp RMSD jumps or systematic drift confirms the stability of the protein-ligand complex and the absence of ligand dissociation during the simulation time.

IUPAC Compound Names

MB_2
{6-[6-(4-methylpiperazin-1-yl)-1H-1,3-benzodiazol-2-yl]-1H-1,3-benzodiazol-2-yl}methanamine

MB_2(Ac)
N-({6-[6-(4-methylpiperazin-1-yl)-1H-1,3-benzodiazol-2-yl]-1H-1,3-benzodiazol-2-yl}methyl)acetamide

MB_2Py(Ac)
N-(5-{6-[6-(4-methylpiperazin-1-yl)-1H-1,3-benzodiazol-2-yl]-1H-1,3-benzodiazol-2-yl}-1-propyl-1H-pyrrol-3-yl) acetamide

MB_3
(6-{6-[6-(4-methylpiperazin-1-yl)-1H-1,3-benzodiazol-2-yl]-1H-1,3-benzodiazol-2-yl}-1H-1,3-benzodiazol-2-yl) methanamine

DB_2P(n)
1) N-({6-[6-(4-methylpiperazin-1-yl)-1H-1,3-benzodiazol-2-yl]-1H-1,3-benzodiazol-2-yl}methyl)-2-(4-{[({6-[6-(4-methylpiperazin-1-yl)-1H-1,3-benzodiazol-2-yl]-1H-1,3-benzodiazol-2-yl}methyl)carbamoyl]methyl}piperazin-1-yl)acetamide
2) N-({6-[6-(4-methylpiperazin-1-yl)-1H-1,3-benzodiazol-2-yl]-1H-1,3-benzodiazol-2-yl}methyl)-3-(4-{2-[({6-[6-(4-methylpiperazin-1-yl)-1H-1,3-benzodiazol-2-yl]-1H-1,3-benzodiazol-2-yl}methyl)carbamoyl]ethyl}piperazin-1-yl)propenamide
3) N-({6-[6-(4-methylpiperazin-1-yl)-1H-1,3-benzodiazol-2-yl]-1H-1,3-benzodiazol-2-yl}methyl)-4-(4-{3-[({6-[6-(4-methylpiperazin-1-yl)-1H-1,3-benzodiazol-2-yl]-1H-1,3-benzodiazol-2-yl}methyl)carbamoyl]propyl}piperazin-1-yl)butanamide
4) N-({6-[6-(4-methylpiperazin-1-yl)-1H-1,3-benzodiazol-2-yl]-1H-1,3-benzodiazol-2-yl}methyl)-5-(4-{4-[({6-[6-(4-methylpiperazin-1-yl)-1H-1,3-benzodiazol-2-yl]-1H-1,3-benzodiazol-2-yl}methyl)carbamoyl]butyl}piperazin-1-yl)pentanamide

$DB_3P(n)$

1) N-[(6-{6-[6-(4-methylpiperazin-1-yl)-1H-1,3-benzodiazol-2-yl]-1H-1,3-benzodiazol-2-yl}-1H-1,3-benzodiazol-2-yl)methyl]-2-[4-({[(6-{6-[6-(4-methylpiperazin-1-yl)-1H-1,3-benzodiazol-2-yl]-1H-1,3-benzodiazol-2-yl}-1H-1,3-benzodiazol-2-yl)methyl]carbamoyl}methyl)piperazin-1-yl]acetamide
2) N-[(6-{6-[6-(4-methylpiperazin-1-yl)-1H-1,3-benzodiazol-2-yl]-1H-1,3-benzodiazol-2-yl}-1H-1,3-benzodiazol-2-yl)methyl]-3-[4-(2-{[(6-{6-[6-(4-methylpiperazin-1-yl)-1H-1,3-benzodiazol-2-yl]-1H-1,3-benzodiazol-2-yl}-1H-1,3-benzodiazol-2-yl)methyl]carbamoyl}ethyl)piperazin-1-yl]propanamide
3) N-[(6-{6-[6-(4-methylpiperazin-1-yl)-1H-1,3-benzodiazol-2-yl]-1H-1,3-benzodiazol-2-yl}-1H-1,3-benzodiazol-2-yl)methyl]-4-[4-(3-{[(6-{6-[6-(4-methylpiperazin-1-yl)-1H-1,3-benzodiazol-2-yl]-1H-1,3-benzodiazol-2-yl}-1H-1,3-benzodiazol-2-yl)methyl]carbamoyl}propyl)piperazin-1-yl]butanamide
4) N-[(6-{6-[6-(4-methylpiperazin-1-yl)-1H-1,3-benzodiazol-2-yl]-1H-1,3-benzodiazol-2-yl}-1H-1,3-benzodiazol-2-yl)methyl]-5-[4-(4-{[(6-{6-[6-(4-methylpiperazin-1-yl)-1H-1,3-benzodiazol-2-yl]-1H-1,3-benzodiazol-2-yl}-1H-1,3-benzodiazol-2-yl)methyl]carbamoyl}butyl)piperazin-1-yl]pentanamide

$DB_3(n)$

1) N,N′-bis[(6-{6-[6-(4-methylpiperazin-1-yl)-1H-1,3-benzodiazol-2-yl]-1H-1,3-benzodiazol-2-yl}-1H-1,3-benzodiazol-2-yl)methyl]propanediamide
5) N,N′-bis[(6-{6-[6-(4-methylpiperazin-1-yl)-1H-1,3-benzodiazol-2-yl]-1H-1,3-benzodiazol-2-yl}-1H-1,3-benzodiazol-2-yl)methyl]heptanediamide
9) N,N′-bis[(6-{6-[6-(4-methylpiperazin-1-yl)-1H-1,3-benzodiazol-2-yl]-1H-1,3-benzodiazol-2-yl}-1H-1,3-benzodiazol-2-yl)methyl]undecanediamide

$DB_2Py(n)$

1) N,N′-bis(5-{6-[6-(4-methylpiperazin-1-yl)-1H-1,3-benzodiazol-2-yl]-1H-1,3-benzodiazol-2-yl}-1-propyl-1H-pyrrol-3-yl)propanediamide
3) N,N′-bis(5-{6-[6-(4-methylpiperazin-1-yl)-1H-1,3-benzodiazol-2-yl]-1H-1,3-benzodiazol-2-yl}-1-propyl-1H-pyrrol-3-yl)pentanediamide
5) N,N′-bis(5-{6-[6-(4-methylpiperazin-1-yl)-1H-1,3-benzodiazol-2-yl]-1H-1,3-benzodiazol-2-yl}-1-propyl-1H-pyrrol-3-yl)heptanediamide
7) N,N′-bis(5-{6-[6-(4-methylpiperazin-1-yl)-1H-1,3-benzodiazol-2-yl]-1H-1,3-benzodiazol-2-yl}-1-propyl-1H-pyrrol-3-yl)nonanediamide
9) N,N′-bis(5-{6-[6-(4-methylpiperazin-1-yl)-1H-1,3-benzodiazol-2-yl]-1H-1,3-benzodiazol-2-yl}-1-propyl-1H-pyrrol-3-yl)undecanediamide
11) N,N′-bis(5-{6-[6-(4-methylpiperazin-1-yl)-1H-1,3-benzodiazol-2-yl]-1H-1,3-benzodiazol-2-yl}-1-propyl-1H-pyrrol-3-yl)tridecanediamide